



LOW VOLTAGE DISTRIBUTION LEVEL THREE TERMINAL UPFC BASED VOLTAGE REGULATOR FOR SOLAR PV SYSTEM

Md. Nasir Uddin¹, M. M. Rashid¹ and N. A. Nithe²

¹Department of Mechatronics Engineering, Faculty of Engineering International Islamic University Malaysia, Kuala Lumpur, Malaysia

²Inspectorate and Electronic Engineering, Dhaka, Bangladesh

E-Mail: nasir.u@live.iiu.edu.my

ABSTRACT

This paper, propose a Three-terminal Reduced DC Bus Capacitance Unified Power Flow Controller (UPFC) for Low Voltage (LV) distribution Networks with High Photovoltaic (PV) penetrations. The device is shown capable of voltage regulating and correcting phase unbalance voltages that can be produced by high levels of distributed photovoltaic (PV) generation. The device is also capable of Power factor improvement (PFI) and correction, regulating the zero, positive and negative sequence voltage in LV distribution Networks and neutral or zero sequence current compensation. Instantaneous reactive power theory shows The power of DC Bus capacitor will fluctuate at twice mains frequency during unbalanced operation. The Real and Instantaneous power balance of Unified Power Flow Controller (UPFC) can be maintained by allowing the shunt input converter to draw a small negative and positive sequence current. The Instantaneous Power balance with negative sequence current allows a hundred-fold reduction in the value of DC bus capacitance which allows long life polypropylene or ceramic capacitors to replace of electrolytic capacitor in this application.

Keywords: UPFC, DC bus capacitance, high PV penetration, LV distribution, instantaneous power theory.

INTRODUCTION

In the form of roof-top domestic systems, the Distributed photovoltaic generation is being installed at an increasing scale. Significant power quality issues, especially voltage rise and voltage unbalance have been widely studied, [1-6]. The penetration of renewable energy supplies in distribution networks is materially restricted by the voltage management philosophies that applied when networks where constructed. For that reason the possibility of large scale PV in the LV distribution networks was not considered. High levels of PV penetration in LV distribution network may alter usual behavior of distribution networks. The majority of distribution networks are radial and the power flow direction is from a point of bulk supply outwards to loads. The operating assumption is that power flows from upstream high voltage networks to the downstream low voltage networks. The single prevailing flow direction allows voltage regulation devices to be set to compensate for the largest voltage drops at the highest loads. The presence of distributed generation can cause the power flow to reverse when the loads are light.[7, 8] In conjunction with the pre-set voltage profile, which is purposefully placed at the upper edge of the acceptable voltage band, distribution over-voltages quickly result. Impacts of high PV penetration include voltage rise, voltage unbalance, and reverse power flow [9-11]. The distribution network demand reduces because a significant portion of power is locally supplied by the installed PV. In some cases, the generation may exceed the feeder loads which will cause the direction of power flow to reverse in the LV

distribution networks [3]. Over-voltages have been observed where high penetrations of residential roof-top solar systems have been installed[7]. In residential districts the midday loads during the working week can be very low while the solar generation is high. The resulting over-voltages cause inverter tripping and the loss of the solar generation. These are the problems which may limit the capacity of distribution networks to absorb PV generation. Consequently voltage regulatory device is necessary to manage the LV distribution network.

THREE TERMINAL UPFC FOR VOLTAGE MANAGEMENT WITH HIGH PV

The studies of literature explore that higher penetrations or renewable generation within the distribution network can be achieved by the addition of intelligent control, regulatory devices and energy storage [12-15]. In this paper Proposed a three terminal UPFC as voltage regulation device for LV distribution networks as shown in Figure-1 which shows a voltage regulation device based on the Unified Power Flow Controller, (UPFC), concept [16]. In this case the DC bus capacitor has a reduced size to allow the application of ceramic capacitors in place of conventional electrolytic capacitors. Electrolytic capacitors often determine the limitations on working temperature for converters and can contribute significantly to cost and failure rate [17, 18]. This paper explores how a three wire UPFC can be controlled if the DC bus capacitor size is reduced by two orders of magnitude – a one hundred fold reduction. Murata, and others now provide high temperature high-current multi-



layer ceramic capacitors, (MLCC), for electric vehicle inverter applications [19]. This paper also demonstrates the performance of voltage regulator with reduced DC bus capacitance. As electrolytic capacitors with thousands of microfarads are replaced by ceramic capacitors of tens of microfarads the major research challenge is to manage the DC capacitor voltage by ensuring instantaneous power balance for the input and output converters [20, 21].

Although, the electrolytic capacitors are the most popular because of its high volumetric efficiency and low cost per unit capacitance, still they suffer from low ripple current capability, short life time, temperature limitations and size [22]. Reduction of DC bus capacitance has the major advantage that allows the application of non-polarised capacitors in place of conventional electrolytic capacitor [17, 23-25].

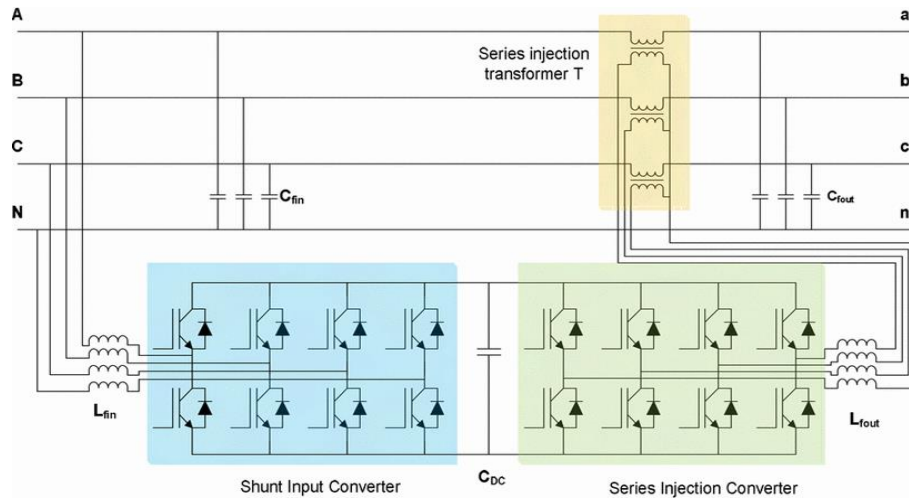


Figure-1. Three terminal reduced DC bus capacitance UPFC based voltage regulator.

DC CAPACITOR VOLTAGE VARIATION AND INSTANTANEOUS POWER FLOWS

In the Figure-1, the proposed UPFC system regulates the voltages at the output terminals a, b and c by injecting a series voltage component. In general low-voltage four-wire distribution networks unbalanced loading or unbalanced solar generation will produce unbalanced variations in voltage. The injected correcting

voltage will have positive, negative and zero sequence components and the series injection converter must have four phase legs to produce the necessary degrees of freedom. Figure-2 shows the regulator system modeled with continuous time voltage and current sources. The instantaneous power developed by the series injection elements is given [2]:

$$ps(t) = ia(t) \times vAa(t) + ib(t) \times vBb(t) + ic(t) \times vCc(t) = ps + \tilde{p} \quad (1)$$

The instantaneous power can be expressed as an average value, p , and an oscillatory component \tilde{p} . The injected voltage is expressed as a sum of positive, negative and zero sequence components.

$$v(t) = \sqrt{2}Vs + (\omega t + \phi_{vs+}) + \sqrt{2}Vs - \sin(\omega t + \phi_{vs-}) + \sqrt{2}Vs0 \sin(\omega t + \phi_{vs0}) \quad (2)$$

$$v(t) = \sqrt{2}Vs + (\omega t - 2\pi/3 + \phi_{vs+}) + \sqrt{2}Vs - \sin(\omega t + 2\pi/3 + \phi_{vs-}) + \sqrt{2}Vs0 \sin(\omega t + \phi_{vs0}) \quad (3)$$

$$v(t) = \sqrt{2}Vs + (\omega t + 2\pi/3 + \phi_{vs+}) + \sqrt{2}Vs - \sin(\omega t - 2\pi/3 + \phi_{vs-}) + \sqrt{2}Vs0 \sin(\omega t + \phi_{vs0}) \quad (4)$$

Similarly the line currents can be expressed as:

$$i(t) = \sqrt{2}Is + (\omega t + \phi_{is+}) + \sqrt{2}Is - \sin(\omega t + \phi_{is-}) + \sqrt{2}Is0 \sin(\omega t + \phi_{is0}) \quad (5)$$

$$i(t) = \sqrt{2}Is + (\omega t - 2\pi/3 + \phi_{is+}) + \sqrt{2}Is - \sin(\omega t + 2\pi/3 + \phi_{is-}) + \sqrt{2}Is0 \sin(\omega t + \phi_{is0}) \quad (6)$$

$$i(t) = \sqrt{2}Is + (\omega t + 2\pi/3 + \phi_{is+}) + \sqrt{2}Is - \sin(\omega t - 2\pi/3 + \phi_{is-}) + \sqrt{2}Is0 \sin(\omega t + \phi_{is0}) \quad (7)$$

The resulting average and oscillatory powers are, [12]:

$$ps = 3Vs + Is \cos(\phi_{vs+} - \phi_{is+}) + 3Vs - Is \cos(\phi_{vs-} - \phi_{is-}) + 3Vs0 Is0 \cos(\phi_{vs0} - \phi_{is0}) \quad (8)$$

$$\tilde{p} = 3Vs + Is \cos(2\omega t + \phi_{vs+} + \phi_{is-}) + 3Vs - Is \cos(2\omega t + \phi_{vs-} + \phi_{is+}) + 3Vs0 Is0 \cos(2\omega t + \phi_{vs0} + \phi_{is0}) \quad (9)$$

Assume the input voltages to the parallel converter are:

$$v(t) = \sqrt{2}Vp + (\omega t + \phi_{vp+}) + \sqrt{2}Vp - \sin(\omega t + \phi_{vp-}) + \sqrt{2}Vp0 \sin(\omega t + \phi_{vp0}) \quad (10)$$

$$v(t) = \sqrt{2}Vp + (\omega t - 2\pi/3 + \phi_{vp+}) + \sqrt{2}Vp - \sin(\omega t + 2\pi/3 + \phi_{vp-}) + \sqrt{2}Vp0 \sin(\omega t + \phi_{vp0}) \quad (11)$$

$$v(t) = \sqrt{2}Vp + (\omega t + 2\pi/3 + \phi_{vp+}) + \sqrt{2}Vp - \sin(\omega t - 2\pi/3 + \phi_{vp-}) + \sqrt{2}Vp0 \sin(\omega t + \phi_{vp0}) \quad (12)$$



In a voltage regulator with negligible energy storage the series injected power must be balanced by power delivered by the shunt converter. It will be shown this can be achieved using positive and negative sequence

currents only. The input currents are arbitrarily controlled in terms of the positive and negative sequence currents as follows:

$$i(t) = \sqrt{2}I_p + (\omega t + \phi_{ip+}) + \sqrt{2}I_p - \sin(\omega t + \phi_{ip-}) \quad (13)$$

$$i(t) = \sqrt{2}I_p + (\omega t - 2\pi/3 + \phi_{ip+}) + \sqrt{2}I_p - \sin(\omega t + 2\pi/3 + \phi_{ip-}) \quad (14)$$

$$i(t) = \sqrt{2}I_p + (\omega t + 2\pi/3 + \phi_{ip+}) + \sqrt{2}I_p - \sin(\omega t - 2\pi/3 + \phi_{ip-}) \quad (15)$$

The parallel input converter instantaneous power is:

$$p(t) = i_A p(t) \times v_{AN}(t) + i_B p(t) \times v_{BN}(t) + i_C p(t) \times v_{CN}(t) = p_p + p_{\tilde{p}} \quad (16)$$

The average and oscillatory powers for the parallel converter are:

$$p_p = 3V_p + I_p + \cos(\phi_{vp+} - \phi_{ip+}) + 3V_p - I_p - \cos(\phi_{vp-} - \phi_{ip-}) \quad (17)$$

$$p_{\tilde{p}} = 3V_p + I_p - \cos(2\omega t + \phi_{vp+} + \phi_{ip-}) + 3V_p - I_p + \cos(2\omega t + \phi_{vp-} + \phi_{ip+}) \quad (18)$$

In practical applications the shunt converter input voltage has a dominant positive sequence component, $V_{p+} < \phi_{vp+}$, but is not necessarily completely balanced. If:

$$V_{p+} \gg V_{p-} \quad (19)$$

Then

$$p_p = 3V_{p+} + I_p + \cos(\phi_{vp+} - \phi_{ip+}) \quad (20)$$

$$p_{\tilde{p}} = 3V_{p+} + I_p - \cos(2\omega t + \phi_{vp+} + \phi_{ip-}) \quad (21)$$

Equation 20 shows that the average power, p , could be satisfied with the lowest current if the shunt converter draws positive sequence current in phase with the local positive sequence voltage. Equation 21 shows the oscillatory power can be balanced by the input converter by drawing a negative sequence current with an appropriate magnitude and phase. These relationships can form the basis of control systems to manage the voltage on a DC bus capacitor with reduced size.

It is noteworthy that the parallel converter can draw a zero sequence current, or a positive sequence reactive current, without producing either an average power term or an oscillatory power term. The zero sequence current magnitude is absent from (20) and (21). For a positive sequence reactive current the phase angle between the voltage and current in (20) is $\pi/2$ resulting in a

zero cosine term. The implication is that the parallel converter can compensate zero sequence current and positive sequence reactive power without any implication for the DC bus capacitor size.

CONTINUOUS DOMAIN COTROL MODEL

Modern switching converters, especially below 100kVA where the switching frequencies often exceed 10 kHz, can be usefully modeled for control purposes using continuous domain models as shown in Figure 2. The series converter is controlled to produce the injected voltages and the parallel converter is current controlled to satisfy the instantaneous power requirements for the series elements.

The DC bus capacitor power is the difference between the input parallel converter power and output series injection powers and the voltage is the integral of the resulting charging current. In the most simplified models it is assumed both converters utilize switching frequencies, filter designs and control methodologies that provide rapid responses that introduce negligible phase delays over the control bandwidths of interest. An improved continuous time model can include the modulation transport delay and the inverter filter state variables.

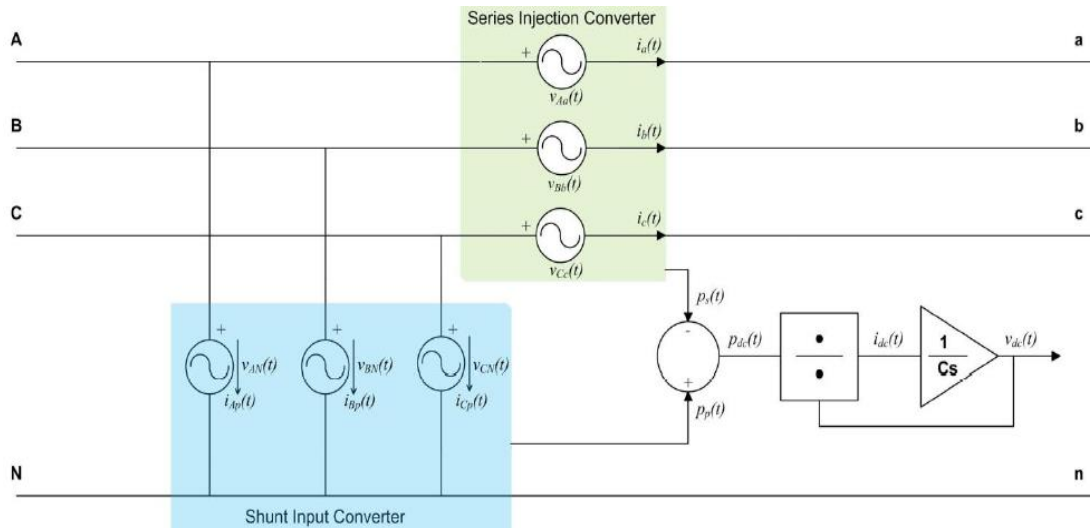


Figure-2. Continuous domain model [2].

The possible voltage control arrangement for the series converter is shown in Figure-3. The series converter is voltage controlled to force the output voltages to follow positive sequence reference set of 230 Vrms. In practice the three controlled voltage source will need to inject positive, negative and zero sequence component. As three degrees of freedom are required with a four leg converter of three independent single phase inverters can be applied. Figures 3 and 4 shows possible control arrangements for the management of the series and parallel converter. The parallel converter must be controlled to provide the instantaneous power demands of the series injection element.

Figure-4 shows a possible power control solution which requires the parallel converter to be equipped with a responsive current control system. An instantaneous power control system could be constructed in the α , β but this paper proposes a positive and negative sequence framework approach. Direct control of the 2ω oscillatory powers in the α , β frame will produce fundamental and third harmonic line currents. This is avoided in the positive/negative sequence based approach. As seen in equation 20 the average power is best satisfied through the

control of an in phase positive sequence current. In figure 4 the average power control system has three parts:

- A feed forward control which calculates the required positive sequence current from the 10ms average power demand of the series converter and the magnitude of the input positive sequence voltage;
- A DC capacitor average voltage control loop that responds to errors in the average DC bus voltage. The controller $G_{cdc}(s)$ has a PI response;
- An instantaneous DC bus voltage limit function. The controller $G_{cinst}(s)$ could have a proportional or hysteresis response. During transients this controller may demand short bursts of positive sequence current that persist for a few milliseconds.

These three systems produce a total positive sequence magnitude demand signal that is multiplied by a three phase positive sequence sinusoidal reference set to produce phase demand signals. The reference set is generated from the converter input voltages using a PLL. The oscillatory 2ω power control loop balances the oscillatory powers introduced by unbalanced loading of the series converter.

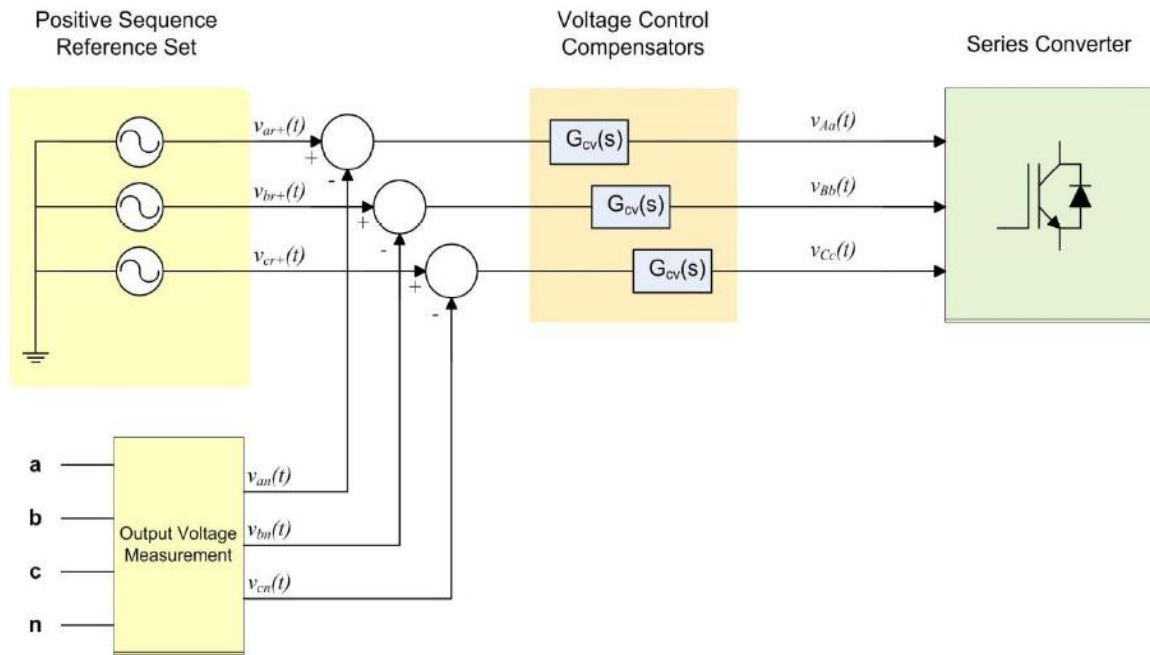


Figure-3. Voltage control management for the series element [2].

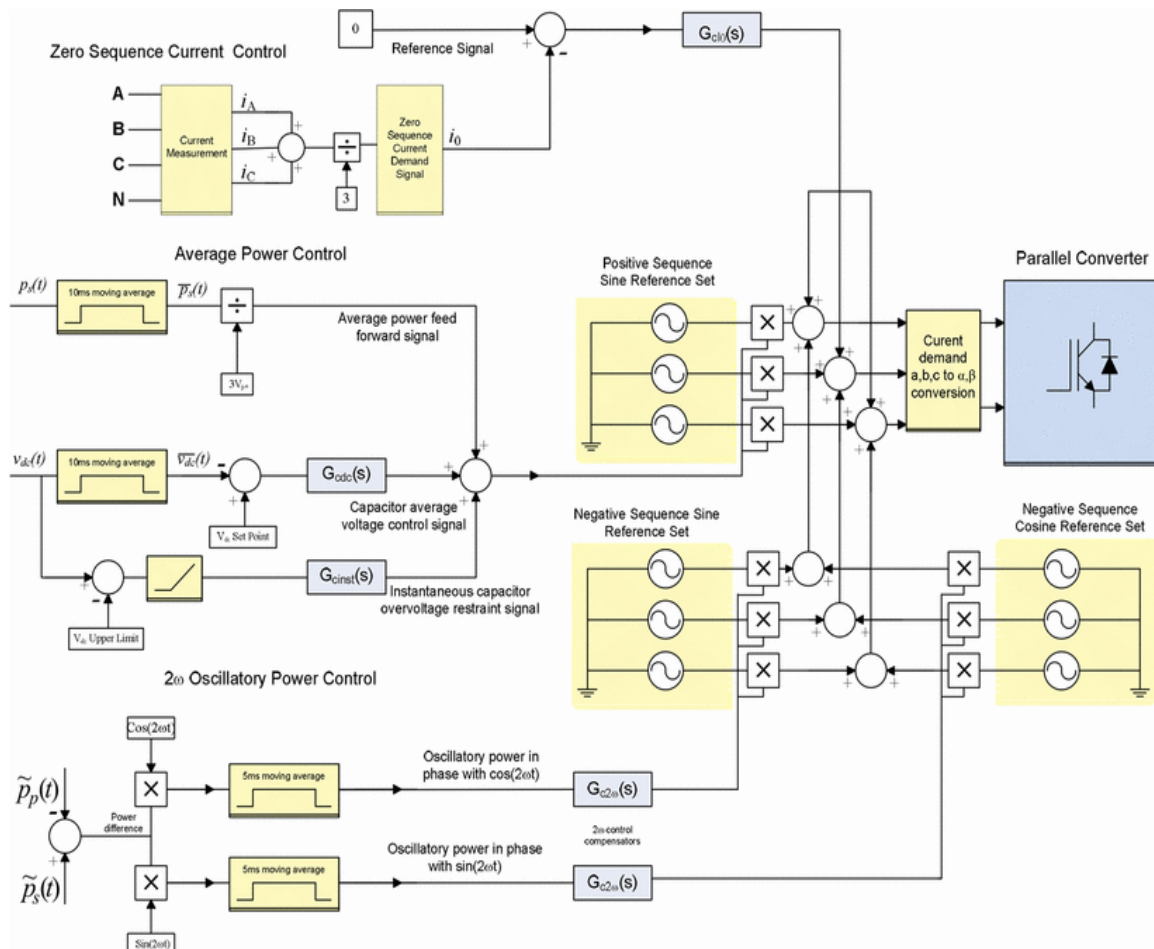


Figure-4. Power control management for the parallel element.



In Figure-4 the instantaneous power difference between the series and parallel converters is determined by subtraction. A sine and cosine synchronous detector and the associated 5ms moving average filters determine the oscillatory powers at 2ω . These components are forced to zero by the actions of the control amplifiers $Gc2\omega(s)$. A residual oscillatory power in phase with $\cos(2\omega t)$ is cancelled by injecting a sinusoidal negative sequence current into the phase current demand signals driving the parallel converter.

FEEDER MODEL WITH UPFC REGULATOR

In the Figure-5 shows a Three-Terminal UPFC orvoltage compensator placed at the centre point of a 300m low voltage four-wire three-phase aerial feeder constructed with a 7/3.75mm all aluminum conductor. The conductor impedance is $(0.452+0.270j)\Omega/\text{km}$. The supply transformer is rated at 200kVA, 415/240V, 50Hz and has a per-unit series impedance of $0.01+0.03j\Omega$. Three 100Arms0.95pf lagging loads are applied to the far end of the feeder. A switchable 50Arms unity power factor single-phase solar generator is also placed at the far end and is connected to phase "b".

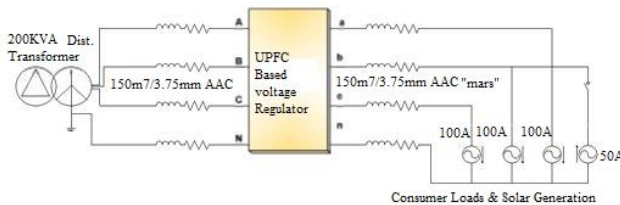


Figure-5. Regulator application in a LV feeder [2].

The key simulation parameters are as follows:

- DC bus capacitor $10\mu\text{F}$; VdcSet Point 700V; VdcUpper Limit 800Vdc;
- DC bus regulator $G_{dc}(s)=0.0004+0.004/s$;
- Output voltage regulators - $G_{ccv}(s)=2+10,000/s$; The three phase reference set has a 240Vrms magnitude; the series injection controlled voltage sources have unity gain;
- Zero sequence current compensator- $G_{cI0}(s)=0.4+8000/s$
- C bus instantaneous voltage limit regulator, proportional gain only above 800Vdc - $G_{cinst}(s)=0.1$; Current limit 10A peak.
- 2ω oscillatory power compensators - $G_{c2\omega}(s)=2+200/s$. The $\sin(2\omega t)$ and $\cos(2\omega t)$ sources have unit magnitude.
- The positive sequence sine and negative sequence sine and cosine sets have unit peak magnitude.

- The parallel converter current sources have a Tran's conductance of 1S.
- To improve the stability of the simulation $10\mu\text{F}$ capacitors are connected at the regulator input from terminals A, B, C to N and at the load terminals, phase to neutral.

RESULTS OF SIMULATIONS

Table-1 outlines the steady state regulatory performance of three terminal UPFC based regulator with the solar generation in service. It is noteworthy that this style of loading produces significant zero sequence voltages. These are four times higher than the negative sequence voltages and this outcome is expected from the network sequence diagrams. As expected the regulator, when in the active state, corrects the voltages at the a,b,c,n output terminals and forces the negative and zero sequence voltages nearly to zero. The attenuation is determined by the voltage loop gain. The input positive sequence current increases, as with any regulator, to provide the real power requirement to correct the positive sequence voltage drop.

Table-1. Input and output voltage and current.

Regulator State	Terminals A,B,C,N	Terminals a,b,c,n	Consumer Terminals
Inactive and Solar Generation Enabled	$V_+ = 229.1V_{\text{rms}}$ $\phi_+ = 0.9^\circ$ $V_- = 2.3V_{\text{rms}}$ $\phi_- = 124.2^\circ$ $V_0 = 9.1V_{\text{rms}}$ $\phi_0 = -116.0^\circ$ $I_+ = 83.9A_{\text{rms}}$ $\phi_+ = -21.0^\circ$ $I_- = 16.7A_{\text{rms}}$ $\phi_- = -59.2^\circ$ $I_0 = 16.7A_{\text{rms}}$ $\phi_0 = 60.6^\circ$	$V_+ = 229.1V_{\text{rms}}$ $\phi_+ = 0.9^\circ$ $V_- = 2.3V_{\text{rms}}$ $\phi_- = 124.2^\circ$ $V_0 = 9.1V_{\text{rms}}$ $\phi_0 = -116.0^\circ$ $I_+ = 84.1A_{\text{rms}}$ $\phi_+ = -21.4^\circ$ $I_- = 16.7A_{\text{rms}}$ $\phi_- = -59.2^\circ$ $I_0 = 16.7A_{\text{rms}}$ $\phi_0 = 60.6^\circ$	$V_+ = 218.3V_{\text{rms}}$ $\phi_+ = 1.8^\circ$ $V_- = 4.5V_{\text{rms}}$ $\phi_- = 124.2^\circ$ $V_0 = 18.2V_{\text{rms}}$ $\phi_0 = -116.0^\circ$ $I_+ = 84.1A_{\text{rms}}$ $\phi_+ = -21.4^\circ$ $I_- = 16.7A_{\text{rms}}$ $\phi_- = -59.2^\circ$ $I_0 = 16.7A_{\text{rms}}$ $\phi_0 = 60.6^\circ$
Active and Solar Generation Enabled	$V_+ = 228.4V_{\text{rms}}$ $\phi_+ = 0.9^\circ$ $V_- = 2.4V_{\text{rms}}$ $\phi_- = 123.0^\circ$ $V_0 = 9.1V_{\text{rms}}$ $\phi_0 = -115.9^\circ$ $I_+ = 88.5A_{\text{rms}}$ $\phi_+ = -19.8^\circ$ $I_- = 17.7A_{\text{rms}}$ $\phi_- = -60.4^\circ$ $I_0 = 16.7A_{\text{rms}}$ $\phi_0 = 60.7^\circ$	$V_+ = 240.3V_{\text{rms}}$ $\phi_+ = 0.8^\circ$ $V_- = 0.1V_{\text{rms}}$ $\phi_- = 0^\circ$ $V_0 = 0.4V_{\text{rms}}$ $\phi_0 = 0^\circ$ $I_+ = 84.1A_{\text{rms}}$ $\phi_+ = -21.4^\circ$ $I_- = 16.7A_{\text{rms}}$ $\phi_- = -59.2^\circ$ $I_0 = 16.7A_{\text{rms}}$ $\phi_0 = 60.7^\circ$	$V_+ = 229.5V_{\text{rms}}$ $\phi_+ = 1.7^\circ$ $V_- = 2.3V_{\text{rms}}$ $\phi_- = 126.0^\circ$ $V_0 = 9.1V_{\text{rms}}$ $\phi_0 = -114.1^\circ$ $I_+ = 84.1A_{\text{rms}}$ $\phi_+ = -21.4^\circ$ $I_- = 16.7A_{\text{rms}}$ $\phi_- = -59.2^\circ$ $I_0 = 16.7A_{\text{rms}}$ $\phi_0 = 60.7^\circ$

There is a slight increase in negative sequence current to provide the oscillatory power necessary to eliminate the negative and zero sequence voltages at the regulator output terminals. This has a minor effect on the negative sequence voltage upstream of the regulator. The oscillatory power could be compensated by the parallel converter with a negative or zero sequence current but a



negative sequence choice is preferable from a voltage disturbance perspective.

The dynamic response of the regulator is explored in Figures 6 to 11. The regulator is allowed to settle into steady state operation with a balanced 100A 0.95 power factor load. At $t=0.5067s$, the voltage zero crossing in "b" phase, a 50A solar generator commences operation. The solar current ramps up over one 20ms cycle and reaches its full current at $t=0.5267s$.

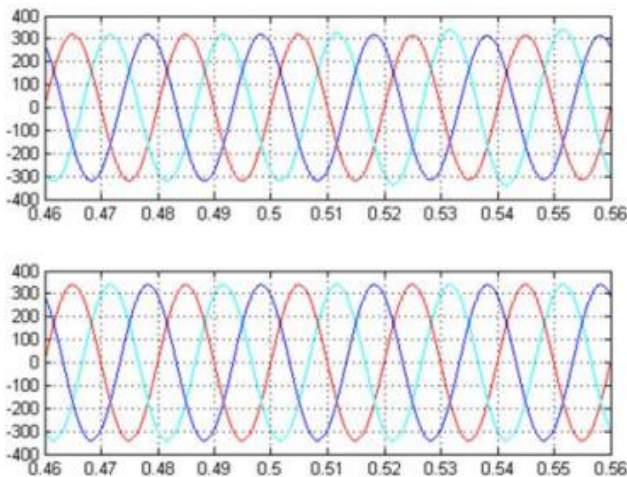


Figure-6. Top traces voltages to N at terminals A, B, C; Lower traces voltages to n at a,b,c.

In the Figure-6 shows the three phase voltages at the input terminals A, B, C and the output terminals a, b, c. The performance of the proposed three-terminal UPFC based voltage regulator is explored in here. It is observed that the voltages at a, b, c output terminals are constant and well regulated. In addition, no variation in output voltage is found when the solar generation enters the network. So overall the output voltages are constant, well regulated and show no variation as the solar generation enters the network. The input voltages prior to $t=0.5067s$ are balanced but low. After the solar generation commences its operation at phase "b", the input voltage at phase "b" (cyan) rises as the phase current reduces.

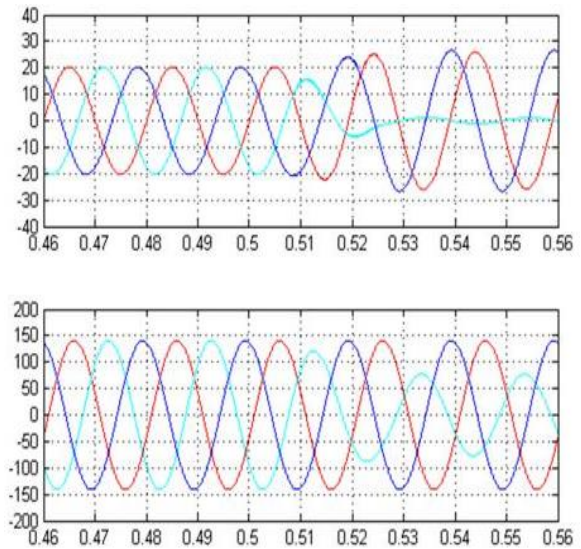


Figure-7. Top traces series injection voltages; lower traces currents from terminals a,b,c,n.

Figure-7 shows the response of the series injection converter. After $t=0.5067s$ the voltage injected in phase "b" (cyan) reduces over one cycle in response to the reduction in phase "b" (cyan) current, seen in the lower trace. Prior to $t=0.5067s$, both the input and output currents are completely balanced and no current flows through the neutral conductor. At $t=0.5067s$, the solar generator commences its operation, the input and output line current becomes unbalanced.

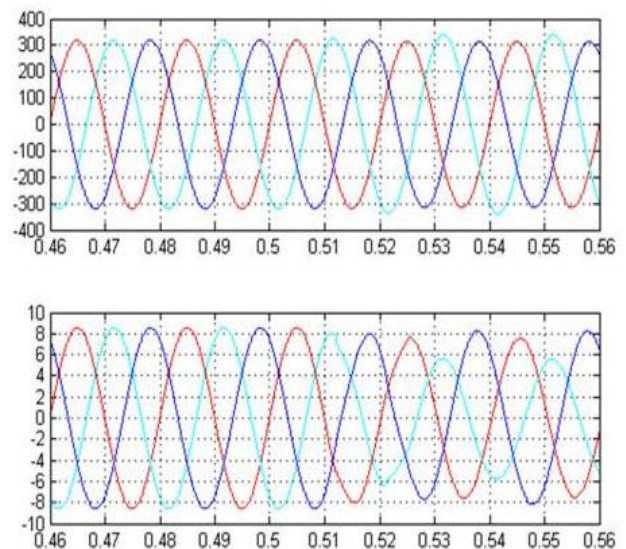


Figure-8. Top traces shunt converter input voltage; lower traces shunt converter input currents.

The response of the series injection converter is shown in Figure-8, which shows the response of the parallel converter. Prior to $t=0.5067s$ the input current is



balanced and the regulator adds a balanced positive sequence voltage to control the voltages at terminals a, b, c. The real power requirement is slightly above 4kW. Once the solar generation starts the real power requirement drops and an oscillatory power requirement develops. The parallel converter draws a combination of positive and negative sequence currents to satisfy the average and oscillatory power requirement.

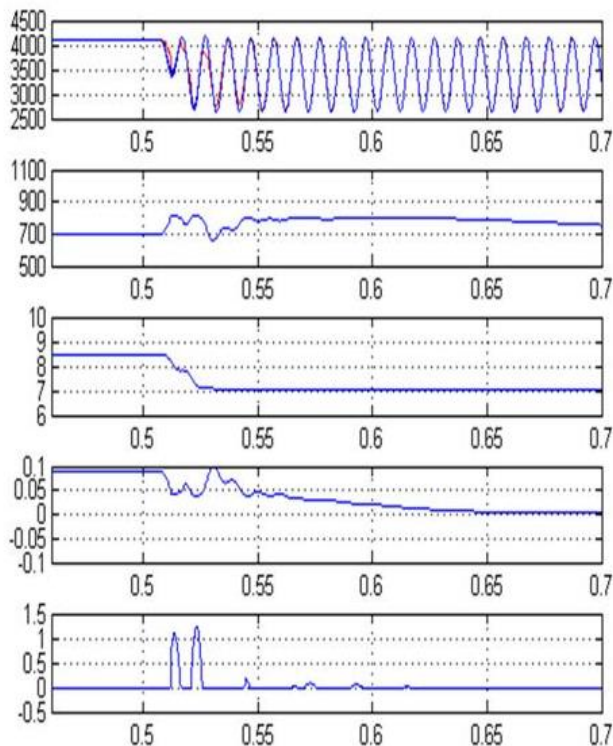


Figure-9. Top traces series converter power (blue) and shunt converter power (red). Other traces top to bottom: DC bus voltage; positive sequence current demand feed forward signal; DC bus voltage regulator current demand; instantaneous bus voltage current demand.

Figure-9 focuses on the positive sequence current control system and the management of the DC bus voltage. As the solar generation commences the line currents become unbalanced and the series converter demands a lower average power and an oscillatory current, shown as the upper blue trace. The parallel converter, the upper red trace, should rapidly follow the power demand to control the DC bus capacitor voltage shown as the second trace.

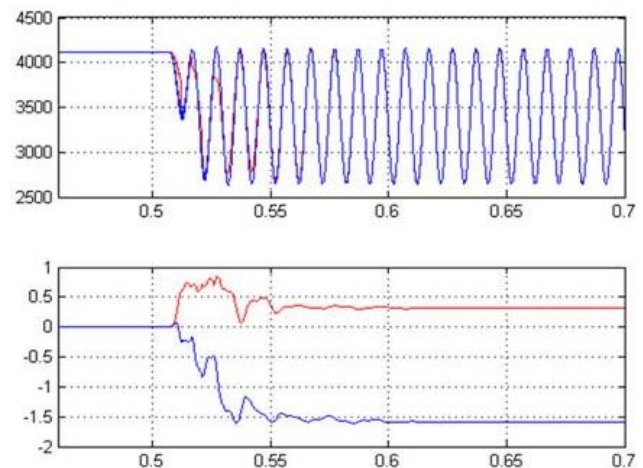


Figure-10. Top traces series converter power (blue) and shunt converter power (red). Lower traces current demand signals for negative sequence cosine (blue) and sine (red) terms.

The positive sequence current forward system has a minimum 10mS response time and the demand signal is shown as the third trace. The capacitor voltage regulation loop, the demand signal of which is shown as the fourth trace, is slow responding and only corrects any minor tracking errors in the feed forward system. The instantaneous power balance causes the capacitor voltage to rise rapidly. Once the capacitor voltage reaches 800Vdc the instantaneous voltage limit system becomes active as shown in the lower trace. This instantaneously reduces the positive sequence current drawn by the parallel converter limiting the voltage rise.

The positive sequence current forward system has a minimum 10mS response time and the demand signal is shown as the third trace. The capacitor voltage regulation loop, the demand signal of which is shown as the fourth trace, is slow responding and only corrects any minor tracking errors in the feed forward system. The instantaneous power balance causes the capacitor voltage to rise rapidly. Once the capacitor voltage reaches 800Vdc the instantaneous voltage limit system becomes active as shown in the lower trace. This instantaneously reduces the positive sequence current drawn by the parallel converter limiting the voltage rise. From $t=0.55$ s the instantaneous loop is inactive and the normal voltage control loop can rebalance the capacitor power and voltage. Figure 10 shows the actions of the 2ω control loops. At $t=0.5067$ s the oscillatory power requirement emerges and the 2ω control amplifiers begin to demand negative sequence sine and cosine currents as shown in the lower traces

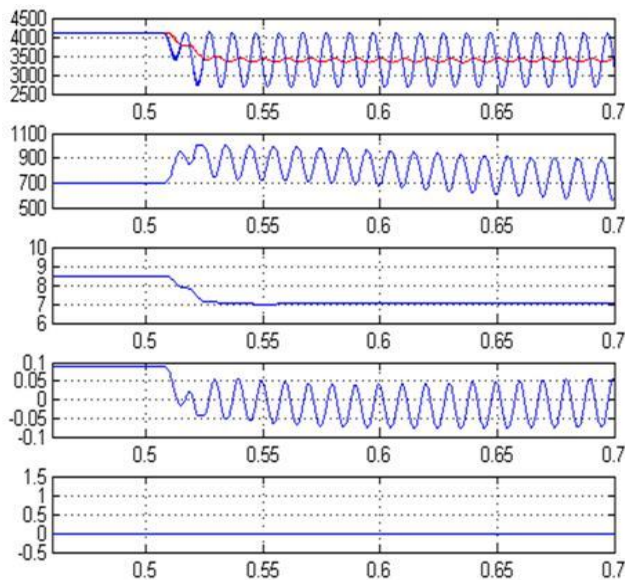


Figure-11. Top traces series converter power (blue) and shunt converter power (red). Other traces top to bottom: DC bus voltage; positive sequence current demand feed forward signal; DC bus voltage regulator current demand; instantaneous bus voltage current demand.

Figure-11 illustrates the effectiveness of the control systems in managing the DC capacitor voltage. In this case the instantaneous voltage limit control system and the 2ω control loops are turned off. From $t=0.5067$ s the parallel converter cannot track the 2ω power oscillations and the DC bus voltage regulators and feed forward systems cannot respond rapidly to the capacitor voltage rise. The DC bus voltage rises sharply and exceeds 1100Vdc, as seen in the second trace. The DC bus average voltage does slowly reduce but the capacitor voltage has a sustained 2ω voltage ripple as the small capacitor is forced to absorb the oscillatory power.

CONCLUSIONS

This paper has established a new method for the management of the DC bus voltage in a distribution level UPFC to allow a hundred-fold reduction in the value of the DC bus capacitance. In this paper, a three terminal UPFC based voltage regulation device for LV distribution networks has been proposed. The output voltages are regulated by injecting series voltages using a four leg converter. Instantaneous reactive power theory has been applied to show how the 2ω power fluctuations that are inherent in the compensation of unbalanced systems can be compensated by allowing the input converter to draw a negative sequence current. The practicality of this approach has been confirmed by a detailed simulation study. The device regulates the positive sequence voltage while eliminating the zero and positive sequence voltages at the output terminals. In the steady state 2ω voltage fluctuations are absent in the DC capacitor voltage as these

are activity suppressed by controlling the shunt converter negative sequence current. During transients the DC bus voltage can be successfully limited by the high speed control of the shunt converter real power through its instantaneous positive sequence current. Simulation results demonstrate that this device actively regulates the voltages at the output terminal and can effectively compensate the zero sequence current of input terminal.

REFERENCES

- [1] P. Wolfs and A. M. T. Oo, "Improvements to LV distribution system PV penetration limits using a dSTATCOM with reduced DC bus capacitance," in Power and Energy Society General Meeting (PES), 2013 IEEE, pp. 1-5, 2013.
- [2] P. Wolfs, "A UPFC with reduced DC bus capacitance for LV distribution networks with high PV penetrations," in Universities Power Engineering Conference (AUPEC), 2012 22nd Australasian, pp. 1-7, 2012.
- [3] M. Alam, K. Muttaqi, and D. Sutanto, "A comprehensive assessment tool for solar PV impacts on low voltage three phase distribution networks," in Developments in Renewable Energy Technology (ICDRET), 2012 2nd International Conference on the, pp. 1-5, 2012.
- [4] F. Shahnia, R. Majumder, A. Ghosh, G. Ledwich, and F. Zare, "Sensitivity analysis of voltage imbalance in distribution networks with rooftop PVs," in Power and Energy Society General Meeting, 2010 IEEE, pp. 1-8, 2010.
- [5] R. Yan and T. K. Saha, "Voltage variation sensitivity analysis for unbalanced distribution networks due to photovoltaic power fluctuations," Power Systems, IEEE Transactions on, vol. 27, pp. 1078-1089, 2012.
- [6] H. Pezeshki, P. Wolfs, and M. Johnson, "Multi-agent systems for modeling high penetration photovoltaic system impacts in distribution networks," in Innovative Smart Grid Technologies Asia (ISGT), 2011 IEEE PES, pp. 1-8, 2011.
- [7] R. Walling, R. Saint, R. C. Dugan, J. Burke, and L. A. Kojovic, "Summary of distributed resources impact on power delivery systems," Power Delivery, IEEE Transactions on, vol. 23, pp. 1636-1644, 2008.



- [8] R. Yan and T. K. Saha, "Investigation of voltage stability for residential customers due to high photovoltaic penetrations," *Power Systems, IEEE Transactions on*, vol. 27, pp. 651-662, 2012.
- [9] K. H. Chua, Y. S. Lim, J. Wong, P. Taylor, E. Morris, and S. Morris, "Voltage Unbalance Mitigation in Low Voltage Distribution Networks with Photovoltaic Systems," 2010.
- [10] F. Shahnia, A. Ghosh, G. Ledwich, and F. Zare, "Voltage unbalance improvement in low voltage residential feeders with rooftop PVs using custom power devices," *International Journal of Electrical Power and Energy Systems*, vol. 55, pp. 362-377, 2014.
- [11] R. Tonkoski, D. Turcotte, and T. H. El-Fouly, "Impact of high PV penetration on voltage profiles in residential neighborhoods," *Sustainable Energy, IEEE Transactions on*, vol. 3, pp. 518-527, 2012.
- [12] R. Tonkoski, L. A. Lopes, and T. H. El-Fouly, "Coordinated active power curtailment of grid connected PV inverters for overvoltage prevention," *Sustainable Energy, IEEE Transactions on*, vol. 2, pp. 139-147, 2011.
- [13] X. Liu, A. Aichhorn, L. Liu, and H. Li, "Coordinated control of distributed energy storage system with tap changer transformers for voltage rise mitigation under high photovoltaic penetration," *Smart Grid, IEEE Transactions on*, vol. 3, pp. 897-906, 2012.
- [14] Y. Zheng, Z. Y. Dong, F. J. Luo, K. Meng, J. Qiu, and K. P. Wong, "Optimal allocation of energy storage system for risk mitigation of DISCOs with high renewable penetrations," *Power Systems, IEEE Transactions on*, vol. 29, pp. 212-220, 2014.
- [15] N. Jayasekara and P. Wolfs, "A hybrid approach based on GA and direct search for periodic optimization of finely distributed storage," in *Innovative Smart Grid Technologies Asia (ISGT)*, 2011 IEEE PES, pp. 1-8, 2011.
- [16] M. A. Sayed and T. Takeshita, "All nodes voltage regulation and line loss minimization in loop distribution systems using UPFC," *Power Electronics, IEEE Transactions on*, vol. 26, pp. 1694-1703, 2011.
- [17] W.-J. Lee and S.-K. Sul, "DC-link voltage stabilization for reduced dc-link capacitor inverter," in *Energy Conversion Congress and Exposition, ECCE 2009. IEEE 2009.*, pp. 1740-1744, 2009.
- [18] J. R. Gazoli, M. de Oliveira F, M. Espindola, T. G. de Siqueira, M. G. Villalva, and E. Ruppert, "Resonant (P+ RES) controller applied to voltage source inverter with minimum DC link capacitor," in *Power Electronics Conference (COBEP)*, 2011 Brazilian, pp. 409-414, 2011.
- [19] C. E. Huggett, L. D. Lewis, R. Rudich, J. L. Scharf, and D. C. Blazej, "Integrated bus bar/multilayer ceramic capacitor module," ed: Google Patents, 1992.
- [20] H. Fujita, Y. Watanabe, and H. Akagi, "Transient analysis of a unified power flow controller and its application to design of the DC-link capacitor," *Power Electronics, IEEE Transactions on*, vol. 16, pp. 735-740, 2001.
- [21] H. Fujita, Y. Watanabe, and H. Akagi, "Transient analysis of a unified power flow controller, and its application to design of the DC-link capacitor," in *Power Electronics Specialists Conference, 1999. PESC 99. 30th Annual IEEE*, pp. 626-631, 1999.
- [22] H. Wang, H.-H. Chung, and W. Liu, "Use of a series voltage compensator for reduction of the DC-link capacitance in a capacitor-supported system," *Power Electronics, IEEE Transactions on*, vol. 29, pp. 1163-1175, 2014.
- [23] H. Wang, W. Liu, and H. Chung, "Hold-up time analysis of a DC-link module with a series voltage compensator," in *Energy Conversion Congress and Exposition (ECCE)*, 2012 IEEE, pp. 1095-1100, 2012.
- [24] W.-J. Lee and S.-K. Sul, "DC-link voltage stabilization for reduced DC-link capacitor inverter," *IEEE Trans Ind Appl*, vol. 50, pp. 404-414, 2014.
- [25] H. Akagi, E. H. Watanabe, and M. Aredes, *Instantaneous power theory and applications to power conditioning* vol. 31: John Wiley and Sons, 2007.